Chemistry–A European Journal
Research Article
doi.org/10.1002/chem.202404712
Chemistry Europe
European Chemical Societies Publishing
www.chemeurj.org

Methyl-π Interactions. Nature of Bonding and Limits of Strength

Steve Scheiner*[a]

Both methyl groups and benzene rings are exceedingly common, and they lie near one another in many chemical situations. DFT calculations are used to gauge the strength of the attractive forces between them, and to better understand the phenomena that underlie this attraction. Methane and benzene are taken as the starting point, and substituents of both electron-withdrawing and donating types are added to each. The interaction energy varies between 1.4 and 5.0 kcal/mol, depending upon the substituents placed on the two groups. The nature of the binding is analyzed via Atoms in Molecules (AIM), Natural Bond Orbital (NBO), Symmetry-Adapted Perturbation Theory (SAPT), nuclear magnetic resonance (NMR) chemical shifts, and electron density shift diagrams. While there is a sizable electrostatic component, it is dispersion that dominates these interactions, particularly the weaker ones. As such, these interactions cannot be categorized unambiguously as either H-bonds or tetrel bonds.

Introduction

Within the kingdom of the H-bond (HB), the strongest are typically those that pair a highly polar proton donor such as an OH group, with a potent electron donor as for example the lone pair of a N atom.[1–7] However, the electrons occupying an aromatic π system can substitute for such a lone pair, even if not quite as readily. And there are indeed a host of OH··π HBs in the literature that are important links in a number of chemical systems and processes.[8–12] Likewise, there is a great deal of literature that has appeared in recent years that has demonstrated that the CH group can serve as proton donor in HBs, even if not typically as strong as those involving OH or NH donors.[13–22]

One might expect the combination of these two partners, viz. a CH··π contact, ought to be exceedingly weak, and perhaps not even attractive enough to merit consideration. Yet such CH··π HBs have been observed in a wide range of systems[19,23–33] in organic and biomolecular chemistry. One example is the field of molecular recognition, as in the case of glucose,[34] saccharides[35] and other species[36] relevant to proteins. The CH··π bond has seen numerous applications in catalysis such as glycoside reactivity,[37] acylation,[38] and the glycosylation of sugars.[39] Some other wide-ranging applications include tunable charge transport[40] organic field effect transistors[41] and efficient and stable Perovskite solar cells.[42,43] Zhou et al[44] have recently noted the superiority of CH··π over π··π interactions for charge transport and conductance for purposes of design of supramolecular materials and devices. To consider a particular small system, benzene dimer is most stable in a T-shape where CH··π interactions are superior to the π-π bonding within a parallel structure.[45,46] Other calculations have demonstrated the importance of CH··π interactions when benzene is combined with cyclohexane.[47,48]

As a special case, the methyl group has the notoriety of being arguably the most common group in all of chemistry. Without the benefit of electron-withdrawing substituents, and with sp^3 hybridization of its C atom, one might expect the simple CH_3 group to be involved in CH HBs in only the most extenuating circumstances. Yet the literature shows this supposition to be incorrect. One forum for such interactions is the broad spectrum of proteins.[49] Surveys of crystals in the CSD and PDB implicate the methyl group as donor to a variety of N and O bases[50–52] or with halide anions.[53] This capacity has been echoed by a series of quantum chemical calculations over the years, mostly involving simple bases rather than an aromatic π-system.[54,55]

Given its chemical composition, the bonding between a methyl group and a Lewis base does not necessarily have to involve a CH HB. There is also the possibility of a tetrel bond (TB) which differs from the HB in that it is the C atom, and not a H center, which serves as the electron acceptor site.[56–64] In the language of molecular orbitals, the σ*(CR) antibonding orbital of Scheme 1 would substitute for σ*(CH) as the charge receptor in a TB versus a HB. From an electrostatic perspective, a σ-hole based on a C atom would interact directly with the base, rather than the positively charged H atom. Such CH_3 tetrel bonds have

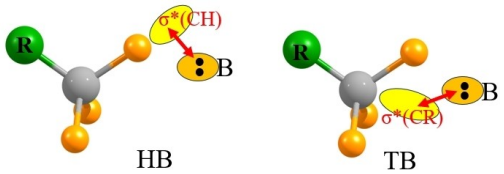

Scheme 1. Cartoon depicting distinction between a HB and TB in the context of a base B interacting with a methyl group.

[a] S. Scheiner
Department of Chemistry and Biochemistry, Utah State University, Logan, Utah 84322-0300, USA
E-mail: steve.scheiner@usu.edu

Supporting information for this article is available on the WWW under https://doi.org/10.1002/chem.202404712

engendered a certain amount of study in the past.[51,54,65–72] Their strength can be as high as 7.6 kcal/mol with a suitably strong base,[70] even higher, near 20 kcal/mol, if the methyl group is part of a cation.[73] Quantum chemical calculations have attempted to devise means to differentiate a methyl TB from a HB on spectroscopic grounds,[74–76] with moderate success to date.

There thus remains a great deal more to be learned about the interaction between a methyl group and a benzene ring. This work examines this question from the framework of quantum chemical calculations. Starting from the very basic system combining methane with benzene, substituents are placed on each subunit so as to explore the full domain of this interaction. Substituents of both electron-withdrawing and donating capacity are added to each, and each dyad is analyzed in a number of ways to probe the energetics and the nature of the binding. It is shown also how the proper placement of such substituents can fully reverse the natural direction of charge flow between the two subunits without necessarily reducing the binding energy. A question that is broached here is whether the interaction would be more appropriately categorized as hydrogen or tetrel bonding.

Methods

Full optimizations were performed at the M06-2X/def2TZVP level of theory[77–79] using the Gaussian 16 (Rev. C.01) package.[80] Harmonic frequency analysis confirmed their nature as true minima. M06–2X has been repeatedly assessed to be one of the most accurate functionals for noncovalent interactions.[81–89] Interaction energies were computed as the difference between the energy of the optimized dyad and the sum of the monomer energies, while in the geometries they adopt within the dimer. This quantity was corrected by the standard counterpoise protocol.[90] The MEP (molecular electrostatic potential) was analyzed to identify the extrema on the 0.001 au electronic isodensity contour of the isolated monomers, utilizing the MultiWFN software.[91,92] Using the AIMAll program,[93] the QTAIM topological analysis[94,95] of the electron density added information about interactions between atoms, represented by bond paths and their bond critical points. NBO analysis[96] identified and quantified the interorbital interactions within dimers. Symmetry-Adapted Perturbation Theory (SAPT) decomposition of the interaction energy[97,98] into its components at the SAPT0 level was carried out via the PSI4 set of programs.[99] NMR calculations employed the gauge-invariant atomic orbital approximation.[100,101]

Results

As a prototype system, methane was first paired with benzene. Substituents were then added to each of these species. As indicated in Figure 1, R1 was added to the methane in a position lying opposite the ring. A pair of substituents R_2 were added to the benzene ring in *para* positions to one another. The choices for substituents comprised a phenyl ring, CH_3, F, Cl, NH_2, NMe_2, OH, CN, and NO_2 so as to encompass a full range of both electron-withdrawing and donating agents.

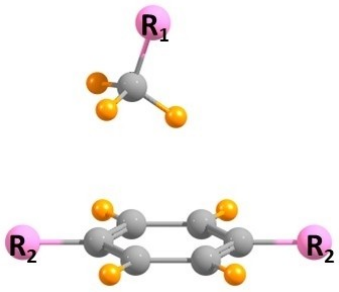

Figure 1. Schematic diagram of the geometry of the complex pairing methane and benzene derivatives, where R_1 and R_2 represent substituents.

Monomers

The molecular electrostatic potential (MEP) that surrounds several of the methane derivatives are illustrated in Figure 2. Of most interest is its positive region, designated by the blue color. There is such a positive MEP near each H of the methyl group, and in many but not all cases a secondary blue region indicating a σ-hole lying opposite the substituent R_1. The magnitude of the positive region is quantified as the maximum V_{max} of the MEP on a 0.001 au isodensity surface. These quantities are listed in Table 1 for both the central C and peripheral H atoms of the methyl group in all of the methane derivatives considered here. It may be noted first that there is no such maximum on the designated surface when the R_1 is either H or a benzene ring Bz. As R_1 becomes progressively more electron withdrawing, this σ-hole appears, and this V_{max},C is competitive with V_{max},H on the H atoms, both rising up to 30 kcal/mol for the strong electron-withdrawing agent NO_2.

The MEPs of benzene and some of its derivatives are displayed in Figure 3. Of greatest relevance is the region above the ring center, which is negative/red in most cases. As may be seen in most of these diagrams, there is a small indentation of

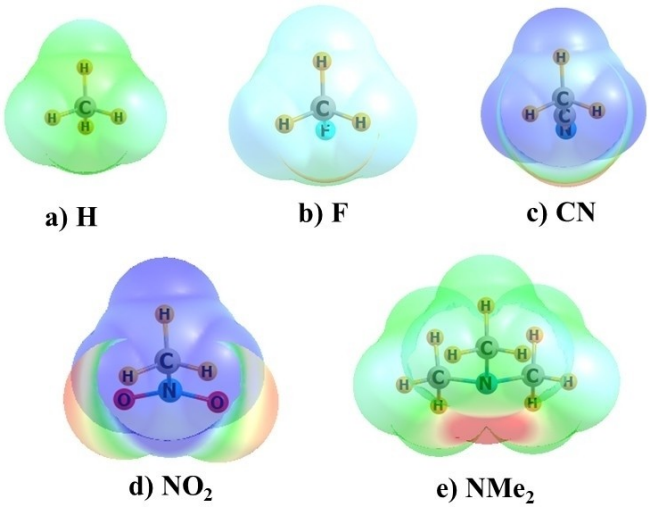

Figure 2. Molecular electrostatic potential (MEP) surrounding selected methane derivatives, where blue and red colors indicate positive and negative MEP, respectively, ±30 kcal/mol.

Table 1. MEP maxima of methane derivatives, in kcal/mol.

R_1	V_{max}, C	V_{max}, H
H	–	8.9
Bz	–	12.1
NMe_2	3.4	10.0
F	20.2	17.9
Cl	20.0	17.2
CN	23.2	28.4
NO_2	29.3	29.9

Table 2. MEP extrema of p-disubstituted benzene derivatives (kcal/mol) and distance d between minimum and axis perpendicular to ring center (Å).

R_2	V_{min}	d	V_{max}
H	−17.2	0.42	−17.0
CH_3	−19.8	0.27	–
NH_2	−20.6	0.24	−24.5
NMe_2	−25.4	0.32	−25.2
OH	−16.5	0.40	−14.5
F	−5.6	0.90	−3.3
NO_2	12.4	1.26	17.5
6 NO_2	–	–	57.0

sorts at the precise center of the region above the ring. In fact, this central position corresponds to a very shallow maximum in the MEP. The actual minima are displaced a small distance d from the axis perpendicular to the ring and passing through the ring center, as sketched out in Figure 3f for the case of benzene. These distances are contained in Table 2 for all derivatives, along with the values of the central local maximum and its nearby minima. In most cases the MEPs at these two positions are not very different. The displacement of the minimum from the ring center is one factor for the geometries of the dyads described below.

As reported in Table 2, V_{min} above the ring is −17.2 kcal/mol for benzene. Placing a pair of electron-releasing substituents in the para positions as R_2, i.e. CH_3, NH_2, or NMe_2, makes this quantity somewhat more negative, with V_{min} rising in magnitude to as much as −25.4 kcal/mol. The electron-withdrawing F does just the opposite, reducing V_{min} down to only −5.6 kcal/mol. The NO_2 group is even stronger in this respect. Indeed, the latter is such a strong electron-withdrawing agent that it makes the potential above the ring positive throughout. Even more extreme, this minimum vanishes entirely for 6 NO_2 substituents, replaced by a maximum of 57.0 kcal/mol, which might be termed a π-hole.

Complexes

When the methane and benzene derivatives are placed together, the geometry of the ensuing dyad is generally as pictured in Figure 1. In most cases, one of the methyl H atoms lies closest to a position above the ring center, with the C offset by a bit from the center. One factor contributing to this off-center location is related to the displacement of the minimum MEP from the center, as described above. The full geometries of some of these complexes are depicted in Figure 4 within the

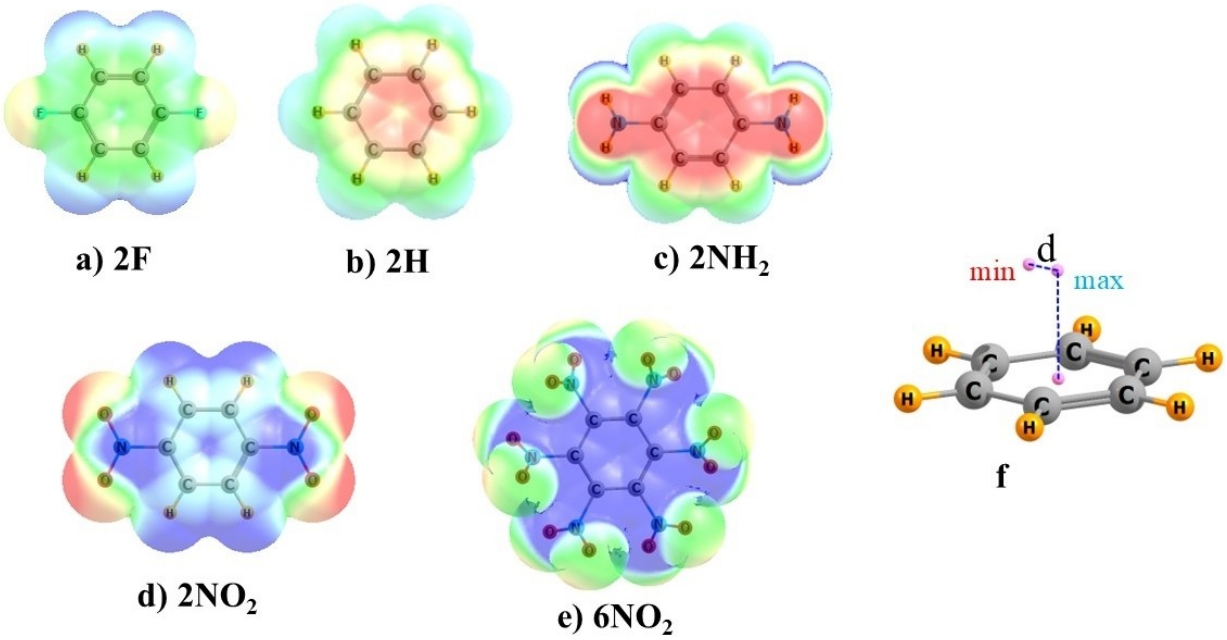

Figure 3. Molecular electrostatic potential (MEP) surrounding selected benzene derivatives, where blue and red colors indicate positive (+25 kcal/mol) and negative (−20 kcal/mol) MEP, respectively. f) positions of maxima and minima lying above molecular plane. Maximum lies directly above ring center and minimum lies a distance d from the perpendicular axis passing through the ring center and the maximum.

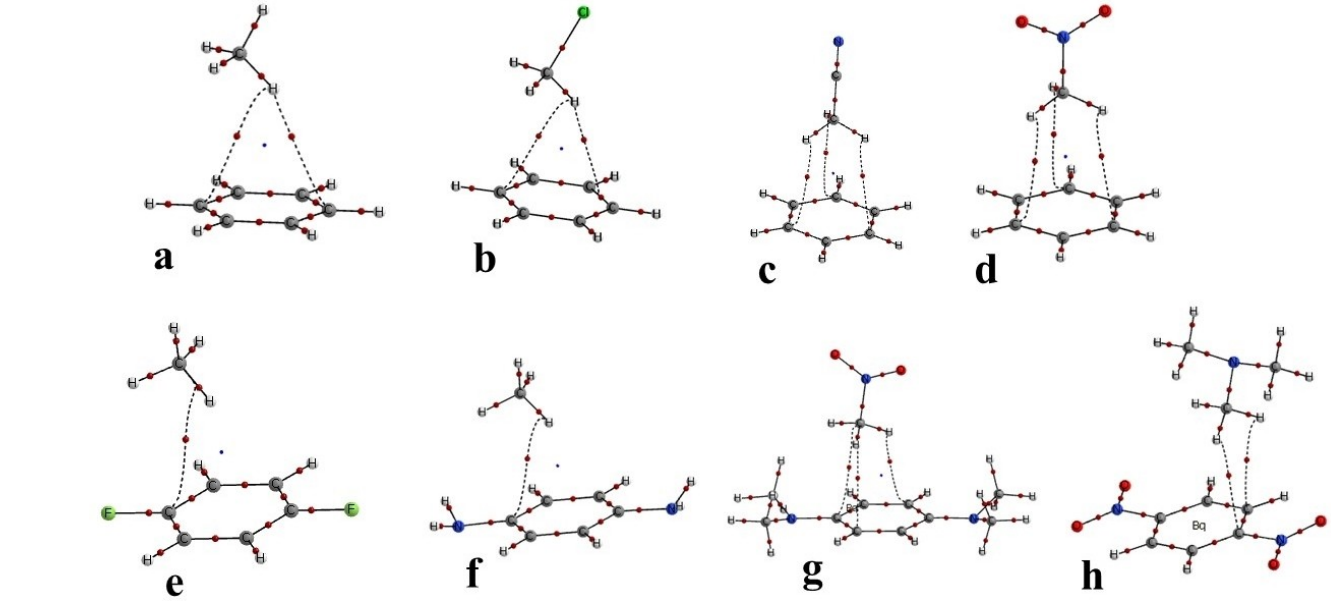

Figure 4. AIM diagrams of complexes pairing benzene with a) methane, b) chloromethane c) cyanomethane and d) nitromethane. Also shown are dyads of e) methane and difluorbenzene, f) methane and diaminobenzene, g) nitromethane and benzene disubstituted with dimethylamine, and h) methane with dimethylamine substituent and dinitrobenzene. Dotted lines indicate bond paths and small red dots show position of bond critical point.

context of an AIM molecular diagram, where intermolecular bond paths are indicated by broken lines. (The cartesian coordinates of all complexes are compiled in the Supporting Information.) A small red sphere occupies the position of the bond critical point of each such path. In most cases, the two monomers are connected by one or more bond paths that connect a methyl H with a phenyl C center. AIM thus diagnoses these interactions as CH··C H-bonds.

The strength of the binding within each dyad is characterized first by the interaction energy, listed as E_{int} in Table 3. These energies follow along with the MEP extrema described in Tables 1 and 2. Specifically, as R_1 becomes more electron-withdrawing, and the V_{max} on the methane derivative grows more positive, the E_{int} grows accordingly. The NO_2 group has the largest effect, more than doubling the interaction energy to 3.1 kcal/mol.

The lower portion of Table 3 documents the way in which electron-releasing substituents on the benzene, which amplify its "π-lump" by making V_{min} more negative, cause the interaction energy to enlarge. This effect is somewhat muted when compared to variations within the comparable methane derivative. The addition of a pair of NMe_2 groups enhances V_{min} from −17.2 to −25.4 kcal/mol, i.e. by a factor of only 1.5. This substitution raises the interaction energy by a similar degree, from 1.4 to 2.3 kcal/mol. The highest degree of bond intensification occurs via a combination of factors. Placing the electron-withdrawing NO_2 on the methane, coupled with the electron-donating NMe_2 substituents on the benzene, ramps up the interaction energy to 5.00 kcal/mol.

The AIM data reflects these bonding patterns to some degree. The second column of data in Table 3 reports the sum of the densities of all bond critical points connecting the two molecules. This density sum amounts to 0.0110 au for the simple methane-benzene pair, and rises and falls along with interaction energy. $\Sigma\rho_{BCP}$ reaches a peak of 0.0211 for the complex pairing nitromethane with the p-disubstituted benzene containing NMe_2 substituents. The correlation between these two measures of bond strength is imperfect, with a linear correlation coefficient of 0.64.

The emphasis to this point has been placed on the interaction between the positive MEP of the methane and the

Table 3. Interaction energy (kcal/mol), sum of AIM bond critical point densities in dyads (10^{-4} au), charge transfer from B to M units (me), and corrected change in proton and C chemical shielding (ppm).

R_1	R_2	E_{int}	$\Sigma\rho_{BCP}$	CT	$\Delta\sigma_H$[c]	$\Delta\sigma_C$[c]
H	H	−1.42	110	1.6	−0.41	−0.90
Bz	H	−1.36	139	1.6	−0.38	0.06
F	H	−2.61	122	1.7	−0.25	−1.67
Cl	H	−2.66	127	2.5	−0.39	−1.43
CN	H	−2.77	157	3.2	−0.63	1.64
NO_2[b]	H	−3.06	159	2.5	−0.45	−1.26
H	F	−1.40	59	1.7	−0.20	−1.10
H	OH	−1.67	63	2.2	−0.35	−1.11
H	CH_3	−1.75	118	1.5	−0.50	−0.57
H	NH_2	−1.84	65	3.2	−0.48	−1.09
H	NMe_2	−2.27	126	2.7	−0.61	−2.93
NO_2	NMe_2	−5.00	211	8.8	−0.69	−2.46
NMe_2	NO_2	−1.46	127	−3.9	−0.11	−1.81
NMe_2[b]	6 NO_2	−3.49	200	-2.4	−0.10	1.53

[a] one small negative frequency referring to Me rotation for R_2=R_3=H. [b] c-C–N held linear, where c refers to center of aromatic ring. [c] Δσ(H/C)-σ(p) where p refers to position of H/C.

negative MEP of the benzene. But can this phenomenon be reversed? A NMe_2 group on the methane diminishes its V_{max} down to only 3.4 kcal/mol. The MEP above the benzene ring becomes quite positive with disubstitution of NO_2 groups. The interaction energy of this pair of molecules is fairly weak, only 1.46 kcal/mol. But this quantity is doubled to 3.49 kcal/mol if six NO_2 groups are added to the benzene. This hexasubstitution eliminates any minimum in its MEP, and amplifies V_{max} to +57.0 kcal/mol.

The latter two complexes do appear to reverse some of the phenomena that stabilize the other dyads. The total amount of charge transferred from the benzene to the methane derivative is defined as CT. This quantity was calculated as the sum of natural atomic charges on the two subunits. The data recorded for CT in Table 3 shows this quantity rises roughly along with the interaction energy. CT culminates in a transfer of 0.0088 e for the R_1=NO_2, R_2=NMe_2 complex. But it is important to note the reversal of sign for the last two complexes in Table 3 where charge is transferred in the opposite direction, from the methane to the benzene derivative.

The interaction energy computed here for the unsubstituted methane-benzene pair of 1.42 kcal/mol is in superb agreement with an earlier study[84] of this same system, that computed a value of 1.46 kcal/mol at the CCSD(T)/CBS level. Another point of similarity is the prior observation that F substituents on the benzene unit have little effect upon the binding energy, whereas electron-donating groups like CH_3, OH and NH_2 enhance this interaction appreciably. Indeed, raising the number of methyl substituents monotonically increases the interaction energy[102]. Another similarity with the literature emerges for the FCH_3··benzene pair where the interaction energy computed here of 2.6 kcal/mol compares quite favorably with a prior estimate[63] of 2.7 kcal/mol.

With regard to methyl interactions with σ-bases, that between FCH_3 and NH_3 has an interaction energy of 1.8 kcal/mol.[103] Combination of $HOCH_3$ with the weak N base NCH was calculated to be 1.3 kcal/mol, but rose to as much as 2.5 kcal/mol for the somewhat stronger NCNa.[69] The methyl group of $HSCH_3$ binds to an amide O with an interaction energy of 1.9 kcal/mol.[73] There is also some precedent for a C atom to act as electron donor[104–109] as observed for the last two structures in Table 3.

Electron Density Analyses

Another window into the nature of the interaction arises when considering how the two subunits mutually perturb their electron densities. Figure 5 depicts the electron density shifts by subtracting the density sum of the two isolated monomers from the total density of the full dimer. Green and purple regions indicate loss and gain of density, respectively. The diagram of the unsubstituted methane-benzene dimer in Figure 5a shows a polarization of the methane as density is shifted upwards, away from the benzene to accommodate density shifting toward it. The loss of density from the benzene is highlighted by the green regions above it. The same sort of

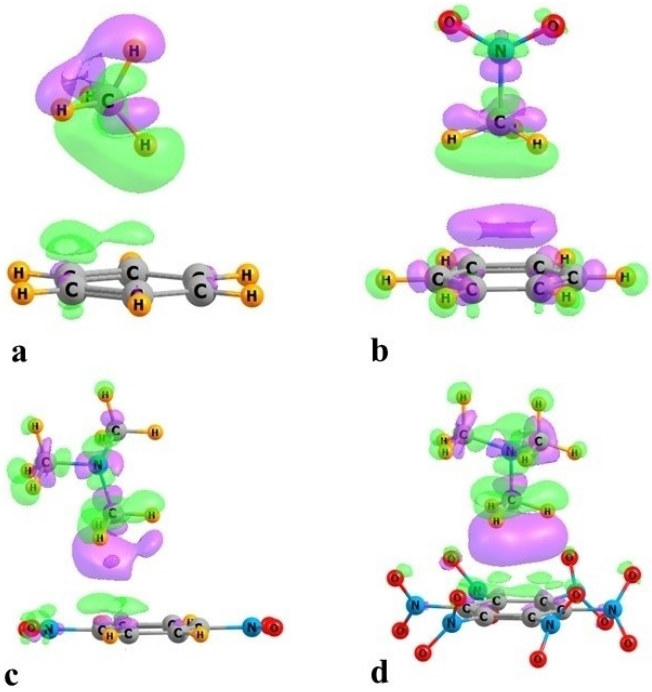

Figure 5. Electron density shifts accompanying formation of complexes of a) methane and benzene, b) nitromethane and benzene, c) dimethylaminomethane and dinitrobenzene, d) dimethylaminomethane and hexanitrobenzene. Purple and green areas denote gain and loss of density, respectively. Contours shown are ±0.0002 au in a and c, ±0.0004 au in b and d.

polarization is seen within the nitromethane of Figure 5b. Along with the much stronger binding, one can see the polarization of the benzene shifting density up toward the electron-accepting nitrobenzene. The reversal of these patterns is evident in Figure 5c which pairs the p-dinitrobenzene with the dimethylaminomethane. There is now a purple charge gain on the underside of the latter molecule, instead of the green charge loss in Figure 5a. This effect is amplified in Figure 5d where the six NO_2 groups on the benzene make for a more potent electron acceptor and a fairly high interaction energy.

The interaction of a methyl group with an electron donor species can typically be interpreted as either a CH··X HB or a C··X tetrel bond directly to the C center. Indeed, there are a number of cases in the literature where confusion as to this issue has arisen. The AIM diagrams in Figure 4 would argue for the HB interpretation as the bond paths emanate from the H atoms, rather than the central C. Whether HB or TB, charge will be transferred from the benzene derivative to the methane, so the amount of CT cannot be used as a litmus test. The NBO procedure provides a more detailed probe, as one can determine whether the charge is moving toward the CH antibonding orbitals as would occur in a HB, or to the CR_1 antibond that would signal a TB. Table 4 helps answer this question by listing E2 for each of these two alternatives, and the answer is a bit more nuanced. It would appear there is a balance between both HB and TB. In general, the TB E2 is larger than that for HB but not by an overwhelming amount. So NBO would suggest there are elements of both sorts of bond, in roughly equal measures.

Table 4. NBO values of E2 (kcal/mol) for transfer from benzene orbitals to methane derivative.

R_1	R_2	TB[a]	HB[b]
H	H	0.18	0.17
Bz	H	0.19	0
F	H	0.45	0.31
Cl	H	0.49	0.23
CN	H	0.17	0.33
NO_2	H	0.51	0.11
H	OH	0.27	0.16
H	F	0.15	0.14
H	CH_3	0.24	0.21
H	NH_2	0.15	0.18
H	NMe_2	0.10	0.12
NO_2	NMe_2	0.70	0.38

[a] transfer into σ*(CR) antibonding orbital. [b] transfer into σ*(CH) antibonding orbital.

A recurring and ubiquitous feature of a HB is the downfield shift of the NMR signal of the bridging proton upon complexation.[110–115] It was found that the methyl protons all shift in the opposite direction, toward greater chemical shielding by 1–3 ppm, when placed above the benzene ring in these various complexes. This upfield shift is easily understandable in the light of the ring currents within the flexible π-electron cloud of the ring, which would have a shielding effect above the ring. In order to remove this overall shielding from that due to the intermolecular interaction itself, the shielding due only to the ring current was computed separately, for only the benzene derivative, at the precise location occupied by the protons of the methane derivative within the complex. This "ring current shielding" was then subtracted from the total change in shielding of these protons that occurs when the methane derivative is placed in confluence with the ring.

These quantities listed in the penultimate column of Table 3 as $\Delta\sigma_H$ can all be seen to be negative. That is, in the absence of the shielding associated with the currents emanating from the ring π-system, these protons would all shift downfield, in accord with expectations for a HB. There is a general pattern of larger downfield shifts accompanying higher interaction energies. For example, the strongest bonding between nitromethane and the benzene with two dimethylamino substituents is associated with the largest shift of −0.69 ppm. But overall, this correlation is only modest at best. Note also that the corrected proton downfield shift is particularly small for the two systems in the last two rows of Table 3, where the direction of charge transfer has reversed. This pattern is sensible as one would expect a charge transfer from ring to methyl to interfere with the normal HB density flow pattern.

The final column of Table 3 contains the analogous chemical shift data for the methyl C nucleus. Like the proton, in all cases, the shielding rises when the Lewis acid is placed in proximity to the aromatic base. But in most cases, this shielding rise is smaller than is caused simply by the presence of the induced field of the aromatic ring current at that position, leading to negative values, tantamount to a deshielding caused by the interaction. However, there are exceptions, most notably the MeCN complex with benzene, and the pairing of NMe_2CH_3 with hexanitrobenzene.

Another perspective on H-bonding strength is associated with the stretching mode of the A–H covalent bond in a generic AH··B HB. The frequency of this vibration typically shifts markedly to the red upon HB formation, and the magnitude of this shift is roughly proportional to the strength of the bond.[113,116–118] The application of this concept to the methyl group of interest here is quite nettlesome, due to the mixing of the three C–H stretching motions which result in a complex mixture of symmetric and asymmetric modes, none of which can be clearly associated with the CH that is most tightly connected with a putative HB.

Still another perspective on the nature of the binding arises if the total interaction energy is decomposed into its constituent elements. Such a decomposition by the SAPT protocol leads to the components listed in Table 5 as electrostatic (ES), exchange repulsion (EX), induction (IND) and dispersion (DISP). Perusal of the data indicates that the electrostatic element lies between 1 and 5 kcal/mol. The induction energy is quite small, accounting for less than 1.5 kcal/mol, but it is the dispersion that is largest of all. DISP accounts for 3.4 kcal/mol in even the weakest complexes at the top of Table 5, and rises to nearly 8 kcal/mol for the bottom row.

The last three columns of Table 5 comprise the percentage contribution of each component to the total of the three attractive elements. ES accounts for between 16% and 43% of this total, which is dwarfed by DISP and its contribution of at least half, and as much as 73% of this sum. There is a general pattern that the percentage contribution of ES rises as the total binding increases, coupled with a diminution of the DISP percent. This pattern is evident in Figure 6 which plots the various percentage contributions against the total interaction energy. There is one somewhat anomalous set of values in Figure 6, for an interaction energy of 3.5 kcal/mol, where the blue and green points lie well off of the correlation line. These values correspond to the system involving the hexanitrobenzene in the last row of the tables. The discrepancy from the other trends, with its anomalously small ES percentage and a high dispersion, is likely related to the direction of charge transfer, opposite to that in the other systems. The ES term is particularly small since there is no V_{min} in this highly substituted benzene derivative which might interact favorably with the maxima in the methane derivative. The dominance of the dispersion term is consistent with prior studies, for example in the pairing of benzene with cyclohexane.[48] This idea extends also to more general types of tetrel bonds where dispersion plays a role comparable to that of electrostatics in certain instances.[119]

Given the diversity of factors contributing to the overall interaction energy between these units, it is worth considering how well any correlate with E_{int}. Of all these factors, the best fit occurs with the induction component of the interaction energy,

Table 5. SAPT components (kcal/mol) and their percentage contribution to total attractive segment of interaction energy.

R_1	R_2	ES	EX	IND	DISP	%ES	%IND	%DISP
H	H	−1.31	3.74	−0.37	−3.44	25.5	7.3	67.2
Bz	H	−1.33	3.71	−0.33	−3.94	23.8	6.0	70.3
F	H	−2.91	5.13	−0.68	−4.02	38.2	8.9	52.8
Cl	H	−2.91	4.93	−0.72	−4.31	36.7	9.0	54.3
CN	H	−3.01	4.48	−0.63	−3.97	39.6	8.2	52.2
NO_2	H	−3.55	4.69	−0.75	−4.00	42.7	9.0	48.2
H	F	−1.35	3.89	−0.29	−3.57	25.8	5.6	68.5
H	OH	−1.58	4.31	−0.40	−3.92	26.8	6.7	66.4
H	CH_3	−1.54	4.25	−0.44	−4.10	25.3	7.3	67.4
H	NH_2	−1.67	4.61	−0.51	−4.19	26.2	8.0	65.8
H	NMe_2	−1.99	5.55	−0.59	−5.12	25.8	7.7	66.5
NO_2	NMe_2	−5.31	7.40	−1.46	−6.18	41.0	11.3	47.7
NMe_2	NO_2	−1.27	3.87	−0.40	−4.40	20.9	6.6	72.5
NMe_2	6 NO_2	−1.69	6.20	−1.32	−7.75	15.7	12.3	72.0

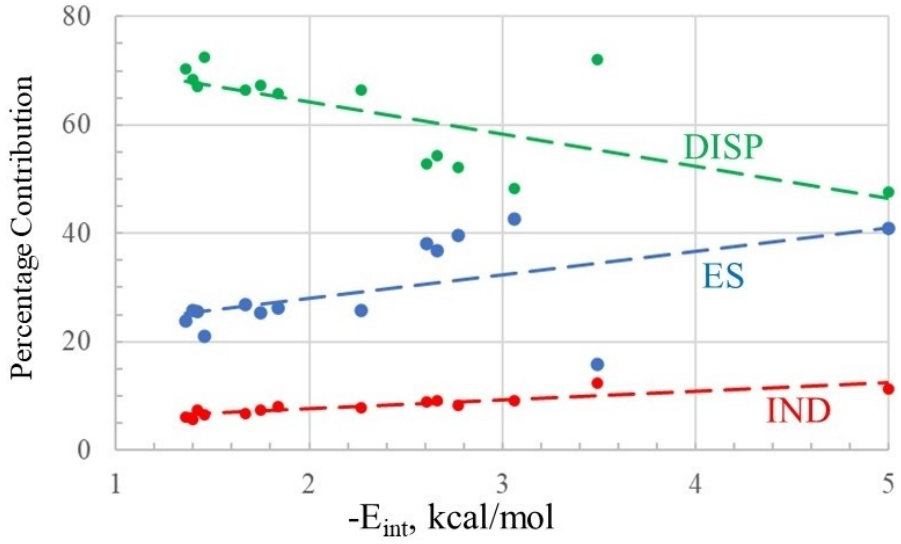

Figure 6. SAPT components as percentage of total attractive sum plotted against full interaction energy.

with a correlation coefficient $R^2 = 0.91$. Correlation with the electrostatic component is poorer, with $R^2 = 0.78$. The sum of bond critical point densities is not an accurate barometer, with a correlation coefficient of only 0.63. None of the other parameters, such as net charge transfer CT, dispersion, and the net deshielding of the bridging proton have correlation coefficients exceeding 0.5. Similarly poor correlations are noted between derived properties. For example, the NMR shift of the proton correlates poorly with the ES component, with $R^2 = 0.30$. It might be thought that perhaps the interaction energy might bear a close relationship with the Hammet constants that are commonly used to understand physical organic reactivities. A linear relationship was noted between E_{int} and Hammet substituent constants σ_p as compiled by McDaniel and Brown[120] for the substituents placed on the aromatic ring. The correlation coefficient here is 0.80.

Conclusions

There is an attractive interaction between a methyl group and a phenyl ring. The binding energy is equal to 1.4 kcal/mol for the simple dyad pairing methane with benzene, but it can be pumped up by appropriate substituents on the two units. An electron-withdrawing group on the methane can amplify its positive electrostatic potential, thereby enhancing its interaction with the negative π-lump above the aromatic ring. The nitro group, for example, doubles this interaction energy, bringing it up to 3.1 kcal. Electron-donating substituents on the ring intensify its π-lump and also raise the binding energy, albeit not as much as the methane substitution. These two effects can be combined. So for example, a nitro group on the methane, coupled with a pair of dimethylamino groups on the benzene, yields an interaction energy of 5.0 kcal/mol. The

binding involves a certain amount of charge transferred from the π-orbitals of the aromatic to the methyl group, but it is possible to reverse this direction by adding nitro groups to the benzene which leads to a strong positive π-hole above the ring. Despite this reversal in transfer direction, the interaction energy remains substantial.

Although Coulombic forces represent a significant component in these methyl-π interactions, it is dispersion which is chiefly responsible for the attraction. The dominating influence of dispersion, particularly in the more weakly bound dyads, would tend to make moot any attempt to classify these interactions as either TB or HB. A more apt description would probably list them as dispersion-dominated, with some assistance from electrostatics, and less still from induction. This categorization helps explain the lack of consistency in the other means of analysis described above. While AIM suggests HBs, a blend of HB with TB arises from NBO treatment of interorbital charge transfer. NMR analysis is not definitive, but is not inconsistent with the idea of H-bonding, although this categorization weakens when the substitutions lead to a reversal in the direction of charge transfer.

Acknowledgements

This material is based upon work supported by the U.S. National Science Foundation under Grant No. 1954310.

Conflict of Interests

There are no conflicts to declare.

Data Availability Statement

The data that support the findings of this study are available from the corresponding author upon reasonable request.

Keywords: H-bond · Tetrel bond · σ-hole · π-lump · Dispersion

[1] G. C. Pimentel, A. L. McClellan, *The Hydrogen Bond*, Freeman, San Francisco **1960**.
[2] K. Luth, S. Scheiner, *J. Phys. Chem.* **1994**, *98*, 3582–3587.
[3] P. Schuster, G. Zundel, C. Sandorfy, *The Hydrogen Bond. Recent Developments in Theory and Experiments*, North-Holland Publishing Co., Amsterdam **1976**.
[4] G. A. Jeffrey, W. Saenger, *Hydrogen Bonding in Biological Structures*, Springer-Verlag, Berlin **1991**.
[5] S. Scheiner, *Hydrogen Bonding: A Theoretical Perspective*, Oxford University Press, New York **1997**.
[6] G. Gilli, P. Gilli, *The Nature of the Hydrogen Bond*, Oxford University Press, Oxford, UK **2009**.
[7] M. M. Szczesniak, S. Scheiner, Y. Bouteiller, *J. Chem. Phys.* **1984**, *81*, 5024–5030.
[8] P. Mastrorilli, V. Gallo, S. Todisco, M. Latronico, G. Saielli, *Chem. Eur. J.* **2016**, *22*, 7964–7969.
[9] A. E. Aliev, J. R. T. Arendorf, I. Pavlakos, R. B. Moreno, M. J. Porter, H. S. Rzepa, W. B. Motherwell, *Angew. Chem. Int. Ed.* **2015**, *54*, 551–555.
[10] M. Saggu, N. M. Levinson, S. G. Boxer, *J. Am. Chem. Soc.* **2012**, *134*, 18986–18997.
[11] J. W. G. Bloom, R. K. Raju, S. E. Wheeler, *J. Chem. Theory Comput.* **2012**, *8*, 3167–3174.
[12] M. A. Muñoz, M. Galán, L. Gómez, C. Carmona, P. Guardado, M. Balón, *Chem. Phys.* **2003**, *290*, 69–77.
[13] R. D. Green, *Hydrogen Bonding by C-H Groups*, Wiley Interscience, New York **1974**.
[14] E. Y. Tupikina, G. S. Denisov, A. S. Antonov, P. M. Tolstoy, *Phys. Chem. Chem. Phys.* **2020**, *22*, 1994–2000.
[15] P. Ramasami, T. A. Ford, *Mol. Phys.* **2018**, *116*, 1722–1736.
[16] S. A. C. McDowell, K. E. K. Edwards, *Mol. Phys.* **2017**, *115*, 3199–3205.
[17] H. I. Rivera-Arrieta, J. M. Turney, H. F. Schaefer, *J. Chem. Theory Comput.* **2017**, *13*, 1478–1485.
[18] Y. Liu, W. Zhao, C.-H. Chen, A. H. Flood, *Science* **2019**, *365*, 159–161.
[19] K. L. Hudson, G. J. Bartlett, R. C. Diehl, J. Agirre, T. Gallagher, L. L. Kiessling, D. N. Woolfson, *J. Am. Chem. Soc.* **2015**, *137*, 15152–15160.
[20] S. Scheiner, T. Kar, *J. Phys. Chem. B* **2005**, *109*, 3681–3689.
[21] J. G. Wasserman, K. J. Murphy, J. J. Newby, *J. Phys. Chem. A* **2019**, *123*, 10406–10417.
[22] A. Bhattacherjee, S. Wategaonkar, *J. Phys. Chem. A* **2017**, *121*, 8815–8824.
[23] M. Nishio, *Phys. Chem. Chem. Phys.* **2011**, *13*, 13873–13900.
[24] M. Nishio, Y. Umezawa, J. Fantini, M. S. Weiss, P. Chakrabarti, *Phys. Chem. Chem. Phys.* **2014**, *16*, 12648–12683.
[25] O. Takahashi, Y. Kohno, K. Saito, *Chem. Phys. Lett.* **2013**, *378*, 509–515.
[26] O. Takahashi, Y. Kohno, M. Nishio, *Chem. Rev.* **2010**, *110*, 6049–6076.
[27] A. Barman, B. Batiste, D. Hamelberg, *J. Chem. Theory Comput.* **2015**, *11*, 1854–1863.
[28] M. J. Plevin, D. L. Bryce, J. Boisbouvier, *Nat. Chem.* **2010**, *2*, 466–471.
[29] K. Ramirez-Gualito, R. Alonso-Rios, B. Quiroz-Garcia, A. Rojas-Aguilar, D. Diaz, J. Jimenez-Barbero, G. Cuevas, *J. Am. Chem. Soc.* **2009**, *131*, 18129–18138.
[30] A. G. Santana, E. Jiménez-Moreno, A. M. Gómez, F. Corzana, C. González, G. Jiménez-Oses, J. Jiménez-Barbero, J. L. Asensio, *J. Am. Chem. Soc.* **2013**, *135*, 3347–3350.
[31] E. G. Baker, C. Williams, K. L. Hudson, G. J. Bartlett, J. W. Heal, K. L. Porter Goff, R. B. Sessions, M. P. Crump, D. N. Woolfson, *Nature Chem. Biol.* **2017**, *13*, 764–770.
[32] Z. R. Laughrey, S. E. Kiehna, A. J. Riemen, M. L. Waters, *J. Am. Chem. Soc.* **2008**, *130*, 14625–14633.
[33] H. K. Ganguly, B. Majumder, S. Chattopadhyay, P. Chakrabarti, G. Basu, *J. Am. Chem. Soc.* **2012**, *134*, 4661–4669.
[34] R. A. Tromans, T. S. Carter, L. Chabanne, M. P. Crump, H. Li, J. V. Matlock, M. G. Orchard, A. P. Davis, *Nat. Chem.* **2019**, *11*, 52–56.
[35] M. d. C. Fernández-Alonso, F. J. Cañada, J. Jiménez-Barbero, G. Cuevas, *J. Am. Chem. Soc.* **2005**, *127*, 7379–7386.
[36] M. W. Krone, C. R. Travis, G. Y. Lee, H. J. Eckvahl, K. N. Houk, M. L. Waters, *J. Am. Chem. Soc.* **2020**, *142*, 17048–17056.
[37] L. Montalvillo-Jiménez, A. G. Santana, F. Corzana, G. Jiménez-Osés, J. Jiménez-Barbero, A. M. Gómez, J. L. Asensio, *J. Am. Chem. Soc.* **2019**, *141*, 13372–13384.
[38] S. A. Blaszczyk, G. Xiao, P. Wen, H. Hao, J. Wu, B. Wang, F. Carattino, Z. Li, D. A. Glazier, B. J. McCarty, P. Liu, W. Tang, *Angew. Chem. Int. Ed.* **2019**, *58*, 9542–9546.
[39] Q. Li, S. M. Levi, C. C. Wagen, A. E. Wendlandt, E. N. Jacobsen, *Nature* **2022**, *608*, 74–79.
[40] H. Jiang, P. Hu, J. Ye, A. Chaturvedi, K. K. Zhang, Y. Li, Y. Long, D. Fichou, C. Kloc, W. Hu, *Angew. Chem. Int. Ed.* **2018**, *57*, 8875–8880.
[41] G. Dai, J. Chang, W. Zhang, S. Bai, K.-W. Huang, J. Xu, C. Chi, *Chem. Commun.* **2015**, *51*, 503–506.
[42] J. Wang, X. Wu, Y. Liu, T. Qin, K. Zhang, N. Li, J. Zhao, R. Ye, Z. Fan, Z. Chi, Z. Zhu, *Adv. Energy Mater.* **2021**, *11*, 2100967.
[43] J. Qi, R. Wang, X. Chen, F. Wu, W. Shen, M. Li, R. He, X. Liu, *J. Mat. Chem. A* **2024**, *12*, 4067–4076.
[44] Y. Zhou, S. Ji, Y. Zhu, H. Liu, J. Wang, Y. Zhang, J. Bai, X. Li, J. Shi, W. Su, R. Huang, J. Liu, W. Hong, *J. Am. Chem. Soc.* **2024**, *146*, 33378–33385.
[45] E. C. Lee, D. Kim, P. Jurečka, P. Tarakeshwar, P. Hobza, K. S. Kim, *J. Phys. Chem. A* **2007**, *111*, 3446–3457.
[46] W. B. Schweizer, J. D. Dunitz, *J. Chem. Theory Comput.* **2006**, *2*, 288–291.
[47] D. B. Ninkovic, D. Z. Vojislavljevic-Vasilev, V. B. Medakovic, M. B. Hall, E. N. Brothers, S. D. Zaric, *Phys. Chem. Chem. Phys.* **2016**, *18*, 25791–25795.
[48] D. B. Ninković, J. P. Blagojević Filipović, M. B. Hall, E. N. Brothers, S. D. Zarić, *ACS Cent. Sci.* **2020**, *6*, 420–425.

[49] V. R. Mundlapati, D. K. Sahoo, S. Bhaumik, S. Jena, A. Chandrakar, H. S. Biswal, *Angew. Chem. Int. Ed.* **2018**, *57*, 16496–16500.
[50] T. J. Mooibroek, *Molecules* **2019**, *24*, 3370.
[51] M. Y. Gusak, M. A. Kinzhalov, A. Frontera, N. A. Bokach, V. Y. Kukushkin, *Chem. Asian J.* **2024**, *19*, e202400421.
[52] R. C. Trievel, S. Scheiner, *Molecules* **2018**, *23*, 2965–2981.
[53] E. Bartashevich, Y. Matveychuk, V. Tsirelson, *Molecules* **2019**, *24*, 1083.
[54] P. Ramasami, T. A. Ford, *J. Mol. Model.* **2022**, *28*, 294.
[55] P. Ramasami, T. A. Ford, *Comput. Theor. Chem.* **2023**, *1220*, 114021.
[56] A. Bauzá, T. J. Mooibroek, A. Frontera, *Angew. Chem. Int. Ed.* **2013**, *52*, 12317–12321.
[57] I. Alkorta, A. C. Legon, *J. Phys. Chem. A* **2024**, *128*, 5963–5968.
[58] I. Bhattacharya, P. Banerjee, *Phys. Chem. Chem. Phys.* **2024**, *26*, 21538–21547.
[59] J. Del Bene, J. Elguero, I. Alkorta, *Molecules* **2018**, *23*, 906.
[60] I. Alkorta, M. M. Montero-Campillo, O. Mó, J. Elguero, M. Yáñez, *J. Phys. Chem. A* **2019**, *123*, 7124–7132.
[61] A. Bauzá, T. J. Mooibroek, A. Frontera, *Chem. Rec.* **2016**, *16*, 473–487.
[62] S. J. Grabowski, *Phys. Chem. Chem. Phys.* **2014**, *16*, 1824–1834.
[63] S. Grabowski, *Molecules* **2018**, *23*, 1183.
[64] S. J. Grabowski, *Phys. Chem. Chem. Phys.* **2017**, *19*, 29742–29759.
[65] A. Daolio, P. Scilabra, G. Terraneo, G. Resnati, *Coord. Chem. Rev.* **2020**, *413*, 213265.
[66] A. Daolio, E. K. Wieduwilt, A. Pizzi, A. Genoni, G. Resnati, G. Terraneo, *Phys. Chem. Chem. Phys.* **2022**, *24*, 24892–24901.
[67] C. Martín-Fernández, M. M. Montero-Campillo, I. Alkorta, J. Elguero, *J. Phys. Chem. A* **2017**, *121*, 7424–7431.
[68] H. Lin, L. Meng, X. Li, Y. Zeng, X. Zhang, *New J. Chem.* **2019**, *43*, 15596–15604.
[69] N. Liu, X. Xie, Q. Li, S. Scheiner, *ChemPhysChem* **2021**, *22*, 2305–2312.
[70] Q. Wu, X. Xie, Q. Li, S. Scheiner, *Phys. Chem. Chem. Phys.* **2022**, *24*, 25895–25903.
[71] B. Suryaprasad, S. Chandra, N. Ramanathan, K. Sundararajan, *J. Phys. Chem. A* **2022**, *126*, 6637–6647.
[72] Q. Wu, X. An, Q. Li, *Mol. Phys.* **2023**, *121*, e2186721.
[73] S. Scheiner, *J. Phys. Chem. A* **2015**, *119*, 9189–9199.
[74] S. Scheiner, *Chem. Phys. Lett.* **2019**, *714*, 61–64.
[75] J. Lu, S. Scheiner, *J. Phys. Chem. A* **2020**, *124*, 7716–7725.
[76] S. Scheiner, *J. Phys. Chem. A* **2018**, *122*, 7852–7862.
[77] F. Weigend, *Phys. Chem. Chem. Phys.* **2006**, *8*, 1057–1065.
[78] Y. Zhao, D. G. Truhlar, *Acc. Chem. Res.* **2008**, *41*, 157–167.
[79] Y. Zhao, D. G. Truhlar, *Theor. Chem. Acc.* **2008**, *120*, 215–241.
[80] M. J. Frisch, G. W. Trucks, H. B. Schlegel, G. E. Scuseria, M. A. Robb, J. R. Cheeseman, G. Scalmani, V. Barone, G. A. Petersson, H. Nakatsuji, X. Li, M. Caricato, A. V. Marenich, J. Bloino, B. G. Janesko, R. Gomperts, B. Mennucci, H. P. Hratchian, J. V. Ortiz, A. F. Izmaylov, J. L. Sonnenberg, D. Williams-Young, F. Ding, F. Lipparini, F. Egidi, J. Goings, B. Peng, A. Petrone, T. Henderson, D. Ranasinghe, V. G. Zakrzewski, J. Gao, N. Rega, G. Zheng, W. Liang, M. Hada, M. Ehara, K. Toyota, R. Fukuda, J. Hasegawa, M. Ishida, T. Nakajima, Y. Honda, O. Kitao, H. Nakai, T. Vreven, K. Throssell, J. A. Montgomery Jr., J. E. Peralta, F. Ogliaro, M. J. Bearpark, J. J. Heyd, E. N. Brothers, K. N. Kudin, V. N. Staroverov, T. A. Keith, R. Kobayashi, J. Normand, K. Raghavachari, A. P. Rendell, J. C. Burant, S. S. Iyengar, J. Tomasi, M. Cossi, J. M. Millam, M. Klene, C. Adamo, R. Cammi, J. W. Ochterski, R. L. Martin, K. Morokuma, O. Farkas, J. B. Foresman, D. J. Fox, Gaussian 16, GAUSSIAN Inc., Wallingford, CT **2016**.
[81] G. Paytakov, T. Dinadayalane, J. Leszczynski, *J. Phys. Chem. A* **2015**, *119*, 1190–1200.
[82] B. S. D. R. Vamhindi, A. Karton, *Chem. Phys.* **2017**, *493*, 12–19.
[83] R. Podeszwa, K. Szalewicz, *J. Chem. Phys.* **2012**, *136*, 161102.
[84] S. Karthikeyan, V. Ramanathan, B. K. Mishra, *J. Phys. Chem. A* **2013**, *117*, 6687–6694.
[85] M. Majumder, B. K. Mishra, N. Sathyamurthy, *Chem. Phys.* **2013**, *557*, 59–65.
[86] M. A. Vincent, I. H. Hillier, *Phys. Chem. Chem. Phys.* **2011**, *13*, 4388–4392.
[87] A. D. Boese, *ChemPhysChem* **2015**, *16*, 978–985.
[88] M. Walker, A. J. A. Harvey, A. Sen, C. E. H. Dessent, *J. Phys. Chem. A* **2013**, *117*, 12590–12600.
[89] L. F. Molnar, X. He, B. Wang, K. M. Merz, *J. Chem. Phys.* **2009**, *131*, 065102.
[90] S. F. Boys, F. Bernardi, *Mol. Phys.* **1970**, *19*, 553–566.
[91] T. Lu, F. Chen, *J. Mol. Graph. Model.* **2012**, *38*, 314–323.
[92] T. Lu, F. Chen, *J. Comput. Chem.* **2012**, *33*, 580–592.
[93] T. A. Keith, *TK Gristmill Software*, Overland Park KS **2013**.
[94] R. F. W. Bader, *J. Phys. Chem. A* **1998**, *102*, 7314–7323.
[95] P. L. A. Popelier, *Atoms in Molecules. An Introduction*, Prentice Hall, Harlow, UK **2000**.
[96] F. Weinhold, C. R. Landis, E. D. Glendening, *Int. Rev. Phys. Chem.* **2016**, *35*, 399–440.
[97] K. Szalewicz, B. Jeziorski, *Molecular Interactions. From Van der Waals to Strongly Bound Complexes* (Ed: S. Scheiner), Wiley, New York **1997**, 3–43.
[98] R. Moszynski, P. E. S. Wormer, B. Jeziorski, A. van der Avoird, *J. Chem. Phys.* **1995**, *103*, 8058–8074.
[99] D. G. A. Smith, L. A. Burns, A. C. Simmonett, R. M. Parrish, M. C. Schieber, R. Galvelis, P. Kraus, H. Kruse, R. D. Remigio, A. Alenaizan, A. M. James, S. Lehtola, J. P. Misiewicz, M. Scheurer, R. A. Shaw, J. B. Schriber, Y. Xie, Z. L. Glick, D. A. Sirianni, J. S. O'Brien, J. M. Waldrop, A. Kumar, E. G. Hohenstein, B. P. Pritchard, B. R. Brooks, H. F. Schaefer III, A. Y. Sokolov, K. Patkowski, A. E. DePrince III, U. Bozkaya, R. A. King, F. A. Evangelista, J. M. Turney, T. D. Crawford, C. D. Sherrill, *J. Chem. Phys.* **2020**, *152*, 184108.
[100] R. Ditchfield, *Chem. Phys. Lett.* **1976**, *40*, 53–56.
[101] R. Ditchfield, R. E. McKinney, *Chem. Phys.* **1976**, *13*, 187–194.
[102] S.-i. Morita, A. Fujii, N. Mikami, S. Tsuzuki, *J. Phys. Chem. A* **2006**, *110*, 10583–10590.
[103] S. Scheiner, *J. Phys. Chem. A* **2017**, *121*, 5561–5568.
[104] A. S. Smirnov, A. V. Rozhkov, M. A. Kryukova, V. V. Suslonov, A. Y. Ivanov, R. M. Gomila, A. Frontera, V. Y. Kukushkin, N. A. Bokach, *Cryst. Growth Des.* **2024**, *24*, 10393–10402.
[105] N. Keshtkar, O. Loveday, V. Polo, J. Echeverría, *Cryst. Growth Des.* **2023**, *23*, 5112–5116.
[106] Y. Chen, L. Yao, F. Wang, *Struct. Chem.* **2024**, *35*, 485–496.
[107] S. Scheiner, *Polyhedron* **2021**, *193*, 114905.
[108] S. Scheiner, *Phys. Chem. Chem. Phys.* **2020**, *22*, 16606–16614.
[109] A. Grabarz, M. Michalczyk, W. Zierkiewicz, S. Scheiner, *ChemPhysChem* **2020**, *21*, 1934–1944.
[110] M. D. Joesten, L. J. Schaad, *Hydrogen Bonding*, Marcel Dekker, New York **1974**.
[111] C. Viragh, T. K. Harris, P. M. Reddy, M. A. Massiah, A. S. Mildvan, I. M. Kovach, *Biochem.* **2000**, *39*, 16200–16205.
[112] V. Dohnal, M. Tkadlecova, *J. Phys. Chem. B* **2002**, *106*, 12307–12310.
[113] R. A. Klein, *J. Comput. Chem.* **2003**, *24*, 1120–1131.
[114] M. A. Kostin, O. Alkhuder, R. E. Asfin, P. M. Tolstoy, *Phys. Chem. Chem. Phys.* **2025**, *27*, 1143–1154.
[115] M. D. A. Montero, F. A. Martínez, G. A. Aucar, *Phys. Chem. Chem. Phys.* **2019**, *21*, 19742–19754.
[116] R. M. Badger, S. H. Bauer, *J. Chem. Phys.* **1939**, *5*, 839–851.
[117] M. D. Joesten, R. S. Drago, *J. Am. Chem. Soc.* **1962**, *84*, 3817–3821.
[118] G. D. Santis, S. S. Xantheas, *J. Chem. Phys.* **2025**, *162*, 044106.
[119] P. R. Varadwaj, A. Varadwaj, H. M. Marques, K. Yamashita, *CrystEngComm* **2023**, *25*, 1411–1423.
[120] D. H. McDaniel, H. C. Brown, *J. Org. Chem.* **1958**, *23*, 420–427.

Manuscript received: December 22, 2024
Accepted manuscript online: February 11, 2025
Version of record online: February 18, 2025